Pergamon

Geochimica et Cosmochimica Acta, Vol. 66, No. 9, pp. 1589–1600, 2002

0016-7037/02 $22.00 + .00

PII S0016-7037(00)00860-2

Microfabric analysis of Mn-carbonate laminae deposition and Mn-sulfide formation in the Gotland Deep, Baltic Sea

IAN T. BURKE and ALAN E. S. KEMP*

School of Ocean and Earth Science, Southampton Oceanography Centre, European Way, Southampton, SO14 3ZH, United Kingdom

(*Received January* 22, 2001; *accepted in revised form November* 7, 2001)

Abstract—The manganese carbonate deposits of the anoxic Littorina sediments of the Gotland Deep have been commonly related to the periodic renewal of deep water by inflowing saline water from the North Sea. The use of scanning electron microscopy–based techniques allows identification of small-scale sedimentary and geochemical features associated with Mn-carbonate laminae, which has significant implications for models of Mn-carbonate formation. Varves occurring in the Littorina sequence contain up to four laminae that may be placed in a seasonal cycle, and kutnahorite laminae occur within varves only as a winter–early spring deposit. This kutnahorite laminae seasonality is in agreement with the seasonal distribution of major Baltic inflow events recorded in historical records, and a direct causal link between inflows and kutnahorite deposition is implied. Benthic foraminifera tests are found to be heavily encrusted in kutnahorite, implying that benthic recolonization during oxidation events occurs concurrently with kutnahorite formation. The relatively common occurrence of small (50 to 100 μm) hexagonal γ-Mn-sulfide pseudomorphs, associated with 13% of kutnahorite laminae studied, is reported in Gotland Deep sediments for the first time. Although Mn-sulfide crystals are not usually preserved in the sediment, the discovery of Mn-sulfide pseudomorphs suggests that initial formation of Mn-sulfide in the Gotland Deep may occur much more commonly during the process of kutnahorite formation than previous reports of Mn-sulfide occurrence have implied.

1. INTRODUCTION

Manganese is insoluble in ocean water with respect to solid Mn(VI) oxides; thus, Mn has a short oceanic residence time. The fate of Mn in the marine environment is therefore largely determined by the redox state of the sediments and bottom waters. Particulate Mn(IV) oxide is normally reduced to soluble Mn(II) as labile organic material is consumed by bacteria (Froelich et al., 1979; Berner, 1981). Because Mn(II) is soluble and released into anoxic water, sediments in these settings would not normally be enriched in Mn (Thomson et al., 1986). However, Mn-carbonate laminae are commonly reported in many organic-rich laminated sediments (Suess, 1979; Hein and Koski, 1987; Okita et al., 1988; Xu et al., 1990; Jenkyns et al., 1991; Fan et al., 1992). Calvert and Pedersen (1993, 1996) proposed that the occurrence of Mn-carbonates in anoxic sediments indicates formation in suboxic conditions under an oxic water column. They have invoked a so-called Mn-pump in which Mn-oxide is supplied from oxic surface sediments and is reduced at depth, producing large in situ Mn^{2+} concentrations leading to pore-water conditions that are supersaturated with respect to a mixed Ca and Mn-rich carbonate, $(Mn_xCa_{1-x})CO_3$. Although previously this phase has been commonly described as Ca-rhodochrosite, in a stricter mineralogical context, this phase is better described as the mineral kutnahorite (Sternbeck, 1997; Böttcher, 1998).

Recent reports of Mn-carbonate in laminated anoxic sediments from Saanich Inlet, British Columbia (Calvert et al., 2001), have been linked to the occurrence of short-lived seasonal flushing events. Such linkage of Mn-carbonate formation to brief oxygenation events is supported by sedimentary and geochemical evidence from the organic carbon–rich Littorina and Modern Baltic sediments of the Gotland Deep (Sohlenius et al., 1996a), where the pervasive presence of discrete authigenic kutnahorite laminae in these sediments is consistent with the formation of kutnahorite in discrete, short-lived, depositional events (Huckriede and Meischner, 1996).

Recent models for kutnahorite formation in the Gotland Deep (Huckriede and Meischner, 1996; Sohlenius et al., 1996a; Neumann et al., 1997; Sternbeck and Sohlenius, 1997) propose a link between the periodic major inflows of oxic saline North Sea water into the brackish Baltic Sea and kutnahorite formation. Normally, there is a strong salinity stratification in the Baltic Sea that effectively inhibits mixing of surface and deep waters (Matthäus, 1990), and the deep waters are prone to anoxia. Bacterially mediated Mn and Fe reduction should consume any Mn- and Fe-oxides supplied to the deep as they sink into the anoxic zone (Froelich et al., 1979). In the anoxic zone, there is then likely to be a decoupling of Mn and Fe deposition (Neumann et al., 1997). Mn^{2+} is soluble in sulfidic waters and can accumulate in the deep anoxic water column (Kremling, 1983; Dyrssen and Kremling, 1990); however, Fe^{2+} reacts quickly with excess free HS^- to form particulate Fe-sulfides and may be stripped from the water column. Fe deposition is limited only by supply of Fe into the Gotland Deep (Boesen and Postma, 1988).

During an inflow event, the Gotland Deep is flushed by saline water, which displaces the anoxic water column upward (Matthäus and Lass, 1995; Neumann et al., 1997). The inflowing water is oxic and rapidly reoxidizes the dissolved manganese present, and large quantities of particulate Mn-oxide are deposited at the sediment–water interface (Heiser et al., 2001).

* Author to whom correspondence should be addressed (aesk@soc.soton.ac.uk).

When all the available oxygen is consumed, these Mn-oxides are then reduced once more, producing high benthic Mn^{2+} concentrations. High benthic Mn^{2+} concentrations in combination with high benthic carbonate alkalinity, produced in situ by bacterial sulfate reduction, can lead to supersaturation with respect to a mixed Mn-Ca-carbonate phase and to the formation of kutnahorite (Huckriede and Meischner, 1996; Sohlenius et al., 1996a; Neumann et al., 1997; Sternbeck and Sohlenius, 1997).

This is an elegant model consistent with much of the reported sedimentary evidence (Huckriede and Meischner, 1996; Sohlenius et al., 1996a; Neumann et al., 1997; Sternbeck and Sohlenius, 1997). The causes of saline inflows are becoming better understood with respect to North Atlantic atmospheric conditions (Matthäus and Schinke, 1994) and environmental variance (Schinke and Matthäus, 1998). If the causal link between major Baltic inflows and kutnahorite laminae could be firmly established, then the use of Mn deposition as a proxy for past saline inflows (and by extension, past North Atlantic climatic conditions) would become possible. To understand the processes involved in the formation of Mn-carbonate–rich laminae, we have used scanning electron microscopy (SEM)–based techniques to study fabric features and lamina scale elemental distributions that may be otherwise be overlooked (by, e.g., bulk chemical analysis) (Brodie and Kemp, 1994; Kemp et al., 1999; Pike and Kemp, 1999).

2. MATERIALS AND METHODS

A 5.64-m gravity core, core 20001-5, was collected in the Central Gotland Deep, 57°13.30 N, 20°04.60 E, in a water depth of 243 m, during cruise 94.44.13.2 of R/V *Alexander Von Humboldt* in August 1994 as part of the Gotland Deep Experiment (Emeis and Struck, 1998) (Fig. 1). Initial core description and subsampling was undertaken by personnel at the Institute of Baltic Research at Warnemünde, where the core was subsampled into 25-cm wet sediment slabs and X-ray exposures were taken. The wet sediment slabs were then vacuum packed in polythene bags to prevent desiccation. Core 20001-5 was dated by lithostratigraphic correlation with other Gotland Deep cores and radiocarbon ^{14}C Accelerator Mass Spectrometry dating performed on a fish bone for Dr. U Struck (Institute of Baltic Research, Warnemünde), with a reservoir correction of -400 yr.

Material analyzed for this study was taken from organic-rich laminated clay gyttja of Littorina age at a core depth of 116 to 143 cm. Sediment samples were prepared for SEM study by fluid-displacive embedding in epoxy resin (Pike and Kemp, 1996; Kemp et al., 1998), allowing thin-section preparation with minimal fabric disturbance. Polished thin sections were prepared by use of an oil-based lubricant, and fabric analysis carried out under the SEM via backscattered electron imagery (BSEI). In addition to BSEI, wet sediment subsamples were prepared for topographical imagery. Nondestructive major element analysis was also performed on thin sections with the energy-dispersive X-ray microanalysis (EDS) tool fitted to the SEM under standard conditions (count time 100 s; excitation volume 2 μm^3; voltage 15 kV; beam current 1×10^{-6} A). Comparison to standard spectra produced quantitative data with errors of less than 10% down to 0.5 wt%. Below 0.5 wt%, errors can increase up to 25%. By use of this technique, the sampled excitation volume can be as little as 2 μm^3, but a 100-μm^2 raster (total excitation volume, 20,000 μm^3) was used to average compositional data over a greater area and produce a better representation of the composition of individual laminae. X-ray diffraction (XRD) analysis of representative samples was performed to establish the range of minerals present. Foraminifera were collected from a single horizon (depth, 117 to 119 cm) by sieving through a 125-μm sieve to remove the clay fraction but retain foraminifera.

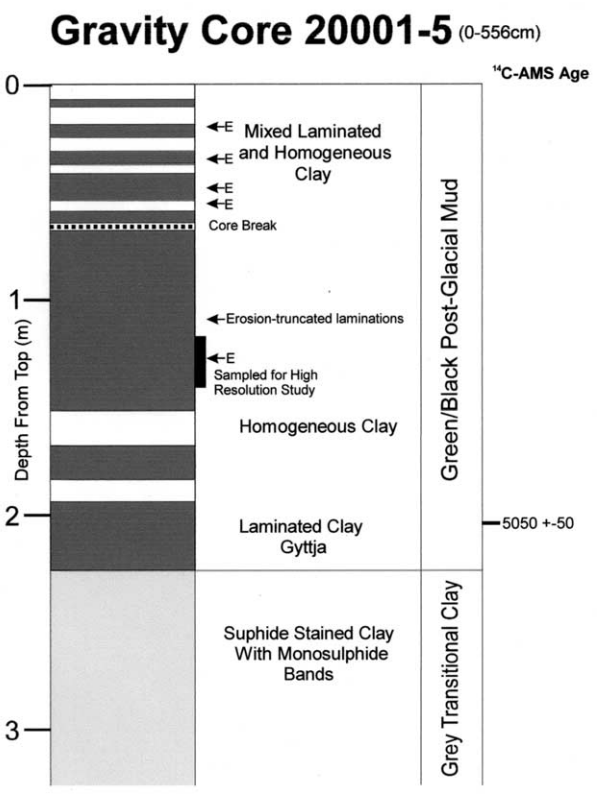

Fig. 1. Lithology of core 20001-5; the interval subsampled for high-resolution study is marked by a black rectangle. The image was logged from X-ray images in Emeis and Struck (1998) by I. T. Burke.

3. BALTIC STRATIGRAPHY

Since the onset of deglaciation, Baltic Sea stratigraphy has been controlled by the balance between global eustatic sea level rise and local isostatic uplift, leading to continual fluctuation of Baltic shorelines and connectivity to the North Sea (Fig. 2). The Late Pleistocene and Holocene (~13 Kyr BP to the present) history and sediments of the Baltic deep are traditionally divided into the five stages summarized in Table 1. Kutnahorite laminae occur throughout the Littorina and Modern Baltic stages.

4. RESULTS AND DISCUSSION

4.1. Annual Succession of Laminae

The Littorina sediments of the Baltic Sea contain intermittently well laminated sequences alternating with indistinctly laminated and bioturbated sequences. In well-laminated sequences, distinct annual cycles of sedimentation, or varves, commonly occur. These varves contain a clear succession of laminae. The spring–summer laminae are represented by dark (under backscattered electron imagery) diatom ooze or as diatomaceous muds containing the frustules of a succession of species characteristic of spring and summer. The late summer–winter deposit is represented by a gray lamina containing terrestrially derived mud, with sparse microfossils (see Burke et al., 2002, for a full discussion of the laminated sediment structure and varve succession model). The presence of varves allows us to place kutnahorite laminae into a seasonal succession of laminae.

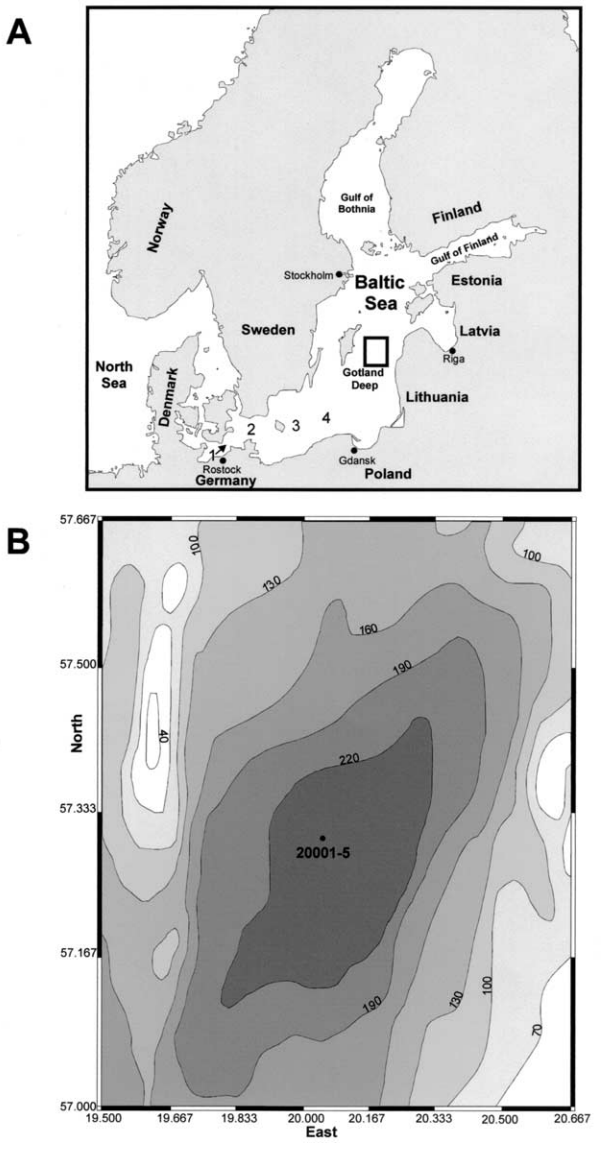

Fig. 2. (A) Map of Baltic Sea showing the locations of the following: 1, Darss Strait; 2, Arkona Basin; 3, Bornholm Basin; 4, Stolpe Channel and the Gotland Deep. (B) Bathymetry of the Gotland Basin (after Emeis and Struck, 1998) and location of core 20001-5

4.2. EDS and XRD Mineralogy

XRD analysis was performed on five representative 1-cm intervals from 116 to 143 cm to determine general mineral composition. All XRD traces show peaks representing the clastic minerals, quartz, illite, and plagioclase feldspar, and kaolinite. Smectite was also indicated in two samples. Kutnahorite was found in two samples by comparison to XRD traces presented in Heiser et al. (2001).

Table 2 shows major element EDS data from a laminated sequence at a core depth of 122 cm containing four distinct varves. Al is used here as a proxy for terrigenous clay and feldspar mineral distribution because these minerals are the only major Al-bearing phases present. Other elements are shown in Figure 3 as X/Al ratios to highlight any variance not due to clay mineral distribution. There is a good correlation between Al and other elements normally associated with clay phases, K (r, 0.97), Mg (r, 0.87), which supports the use of X/Al ratios (Fig. 3A). The annual cycle is reflected in the Al profiles, which have high values in the clay-rich winter deposits of varves 1, 3, and 4, and low values in the diatomaceous spring–summer laminae of varves 1 and 4.

The epoxy resin used to embed these sediments contains only C and Cl and O. Although C and O are both present in mineral phases, Cl is not present in any mineral phase present. Because the resin contains approximately 2 wt% Cl and the resin is the only source of Cl in these sediments, Cl can be used here as an approximate proxy for porosity, with 2 wt% Cl $\approx$ 100% porosity (Fig. 3A). There is a general reduction in porosity in the clay-rich winter deposit in varves 1, 2, and 3, and high porosity in the diatomaceous laminae in varves 1, 3, and 4 because of the open structure of diatom frustules in comparison to clay-rich laminae. Where the large Mn/Al enrichment (>10 times) occurs in kutnahorite lamina C, there is also a marked reduction in porosity. Enrichments in Si/Al are due to the presence of siliceous diatoms in the spring–summer bloom laminae and are observed in all varves (Fig. 3A).

Varves 1, 2, and 3 all contain bright kutnahorite laminae. Large enrichments up to two orders in magnitude in both Mn/Al and Ca/Al occur within these laminae (Fig. 3B). Mn and Ca have a strong positive correlation (r, 0.97) demonstrating that both elements occur together in the same mineral phase (i.e., kutnahorite). Mg/Al is modestly enriched in kutnahorite laminae C (see Fig. 3A), showing that small amounts of Mg are also sequestered in kutnahorite. The kutnahorite laminae occur in the winter terrigenous deposit or straddling the late winter deposit and the early spring diatomaceous deposit. Where kutnahorite laminae occur in varves, they uniquely occur as a winter–early spring deposit.

Fe/Al and S/Al also have a strong positive correlation (r, 0.89) suggesting that Fe is sequestered in these sediments in a sulfide phase (Fig. 3C). Fe/Al shows relatively little variance when compared with that of Mn/Al; this illustrates the possible decoupling of Mn and Fe deposition in this setting. Neumann et al. (1997) proposed that Fe-oxides supplied to the Gotland deep are rapidly reduced and deposited as Fe-sulfides upon entering the anoxic zone, whereas reduced Mn accumulates in anoxic bottom water and is only deposited during discrete events. There are, however, minor enrichments in S/Al within kutnahorite laminae A, B, and D, and Fe/Al in kutnahorite laminae A and D, which may be related to Mn deposition.

Table 3 shows the results of EDS spot analyses (excitation volume, 2 μm^3) on 79 individual kutnahorite crystallites. Although there is much variation in composition, the mean value gives a calculated kutnahorite composition of $(Mn_{0.75}Ca_{0.22}Mg_{0.03}Fe_{0.00})CO_3$, which is in agreement with previous studies (Jakobsen and Postma, 1989; Huckriede and Meischner, 1996). The large range in Cl (wt%) values indicates a large range in porosity for individual grains. Strikingly, kutnahorite is almost completely free of Fe, but not S. The presence of S in kutnahorite has been not been previously reported (Calvert and Price, 1970; Suess, 1979; Pedersen and Price, 1982; Jakobsen and Postma, 1989; Huckriede and Meischner, 1996; Lepland and Stevens, 1998). This S must be sequestered in a contaminant phase hitherto not described

Table 1. Stratigraphic stages of the Baltic Sea.

Baltic stage[a–e] ^{14}C	Sediment type[g]	Organic carbon (wt%)[f]	Salinity (‰)[b]	Fossil assemblage	Environmental conditions
Modern Baltic or Liminea Recent–3 Ka BP	Mixed laminated and homogenous clay gyttja	3.0–5.5	6–9	Brackish water diatoms[b]	Continuation of Littorina stage; however, slow isostatic uplift of sill region led to the restriction of saline inflow, reducing salinity.[a,g]
Littorina (including Mastogloia) 3–8.1 Ka BP	Laminated and homogenous clay gyttja	3.0–5.5	Up to 20	Brackish water diatoms[b]	Initiated by rapid eustatic sea level rise, connection to the North Atlantic established the brackish conditions and salinity stratification that have persisted to the present day.[b] A 2–5% enrichment in manganese is due to the occurrence of kutnahorite laminae.[h]
Ancylus 8.1–9.5 Ka BP	Homogenous sulfide stained clay	1.2	Fresh water	Fresh water mollusc Ancylus fluviatilis[i]	Final lacustrine stage initiated by rapid isostatic uplift.[c,g,i]
Yoldia 9.3–10.0 Ka BP	Glaciogenic microvarved clay	0.4	Approx. 10%	Brackish water diatoms and dwarf marine bivalve Portlandia "Yoldia" arctica[i]	Formed after a catastrophic 25-m drop in lake level down to Yoldia sea level; brackish conditions only persisted for 200–300a during mid-Yoldia times.[d,g]
Baltic Ice Lake 10.0 to approx. 13 Ka BP	Glaciogenic ice marginal varved clay	0.5	Fresh water	Sparse cold-water diatoms[j]	Early ice-damned lake, formed from meltwater from the Weichselian Ice Sheet.[k]

[a] Ignatius et al. (1981).
[b] Sohlenius et al. (1996a).
[c] Björck (1995).
[d] Wastegård et al. (1995).
[e] Björck et al. (1996).
[f] Danyushevskaya (1992).
[g] Mörner (1995).
[h] Huckriede and Meischner (1996).
[i] Zenkevitch (1963).
[j] Kabailiené (1995).
[k] Raukas (1995).

Table 2. Energy dispersive X-ray microanalysis (EDS) data.

Depth (mm)	Al (wt%)	Cl (wt%)	Si/Al	K/Al	Mg/Al	Ca/Al	Mn/Al	S/Al	Fe/Al
0.00	1.36	1.61	3.22	0.35	0.19	0.08	0.34	0.59	0.72
0.10	1.39	1.36	3.58	0.40	0.22	0.35	0.99	1.12	1.16
0.20	0.32	1.67	8.16	0.47	0.28	0.13	1.31	3.03	1.75
0.30	0.69	1.60	5.80	0.39	0.29	0.19	0.55	0.72	0.77
0.40	0.81	1.75	5.36	0.41	0.23	0.06	0.49	0.64	0.78
0.50	1.00	1.92	3.30	0.45	0.21	0.11	0.50	1.18	1.28
0.60	0.99	1.55	3.48	0.43	0.21	0.07	0.40	1.53	1.35
0.70	2.19	1.34	2.78	0.40	0.18	0.09	0.32	0.72	0.89
0.80	2.61	1.12	2.32	0.39	0.19	0.31	1.07	0.64	0.82
0.90	1.24	1.32	4.59	0.40	0.23	0.69	2.75	0.68	0.91
1.00	0.88	1.88	4.43	0.33	0.23	0.38	1.85	0.52	0.61
1.10	1.35	1.34	4.77	0.44	0.21	0.04	0.21	0.26	0.65
1.20	1.26	1.30	4.29	0.32	0.25	0.03	0.25	0.44	1.26
1.30	0.61	1.85	6.77	0.39	0.18	0.02	0.41	0.75	0.92
1.40	0.74	1.60	4.27	0.38	0.23	0.15	0.30	0.65	0.65
1.50	2.05	1.54	2.60	0.37	0.17	0.14	0.31	0.66	0.65
1.60	0.76	0.92	3.28	0.37	0.50	4.86	17.07	1.84	1.24
1.70	1.31	1.32	2.97	0.45	0.28	0.84	5.12	0.76	0.67
1.80	1.18	1.36	3.13	0.37	0.26	0.88	3.57	1.17	0.95
1.90	1.56	1.49	3.17	0.42	0.21	0.14	0.37	0.57	0.85
2.00	1.89	1.39	2.92	0.42	0.20	0.08	0.23	0.95	1.16
2.10	1.91	1.40	3.16	0.35	0.21	0.10	0.37	0.49	0.73
2.20	1.31	0.97	8.01	0.53	0.15	0.08	0.27	0.41	0.61
2.30	1.71	1.27	2.96	0.45	0.22	0.37	1.42	1.29	1.49
2.40	2.03	1.45	2.64	0.41	0.21	0.33	1.23	0.33	0.65
2.50	1.75	0.91	2.58	0.35	0.22	0.26	1.47	2.47	2.39
2.60	2.38	1.38	2.41	0.39	0.22	0.28	1.14	0.39	0.70
2.70	1.68	1.67	3.70	0.39	0.18	0.09	0.40	0.32	0.61
2.80	1.37	1.58	4.66	0.39	0.20	0.13	0.31	0.69	0.81
2.90	1.20	1.57	3.63	0.43	0.21	0.15	0.32	1.28	1.17
3.00	1.16	1.30	4.05	0.41	0.19	0.16	0.50	1.09	0.97
3.10	1.71	1.42	3.46	0.37	0.23	0.15	0.30	0.52	0.62
3.20	2.10	1.49	2.78	0.44	0.19	0.09	0.18	0.54	0.81
3.30	1.93	1.27	2.74	0.38	0.24	0.07	0.67	0.96	0.79
3.40	2.17	1.47	3.06	0.41	0.18	0.06	0.18	0.38	0.62
3.50	1.75	1.33	2.99	0.36	0.20	0.15	0.23	0.87	0.92

within the kutnahorite phase. The compositional data in Table 3 does support a possible Mn-sulfide phase, although with respect to the pore-water conditions prevalent in Gotland Deep, Mn-sulfide would not be expected (Kulik et al. 2000; Heiser et al. 2001). Aller (1980) reports, however, that because of the large range of values reported for the K_{sp} of Mn-sulfide, it is impossible to eliminate the possibility of forming or preserving Mn-sulfide on solubility calculations alone. Aller (1980) also reports that for Long Island Sound sediments, Mn^{2+} concentrations near the sediment–water interface can vary considerably on seasonal timescales; therefore, it is possible that some early Mn-sulfide forms in this setting, and is preserved by inclusion in the kutnahorite lattice.

4.3. Occurrence of Foraminifera

Sparse numbers of benthic and planktonic foraminifera tests were found in Littorina sediments; only 26 foramerifera tests were recovered from 6 cm^3 of sediment. The planktonic species include the following: *Globigerina bulloides* (d'Orbigny), *Globoturborotalia rubescens* (Hofker), *Turborotalita quinqueloba* (Natland), *Neogloboquadrina pachyderma* (Ehrenberg), *Globorotalia scitula* (Brady), and *Globigerinita glutinata* (Egger). The benthic species include *Elphidium excavatum* (Terquem), *Elphidium albiumbilicatum* (Weiss), *Ammonia* sp., *Spiroloculina canaliculata* (d'Orbigny), and *Cassidulina* sp.

The benthic assemblage is typical of that found in the present Baltic Sea (Brodniewicz, 1965); however, any planktonic assemblage is unexpected in this setting because the basin is shallow and brackish, and its waters are rich in suspended matter. The planktonic specimens are all rather small and delicate ($\sim$150 μm) and are unbroken, which implies growth in the Baltic Sea; however, a source from outside the Baltic or from erosion from older sediments cannot be excluded. If erosion of older sediments is the origin of foraminifera tests in this setting, then both benthic and planktonic foraminifera tests should be supplied simultaneously and not have any difference in occurrence. However, there is an intriguing difference in the condition of the surface of planktonic and benthic tests. The tests of all 14 benthic specimens are heavily encrusted in kutnahorite, whereas all 12 planktonic specimens are free of kutnahorite (e.g., Figs. 4A–D). The kutnahorite occurs both on the surface benthic foraminifera test and as fine intergrowths within the test itself (Fig. 4B). It was therefore impossible to sample the benthic foraminifera test composition by EDS spot analysis without kutnahorite contamination.

The difference in kutnahorite encrustation may be explained

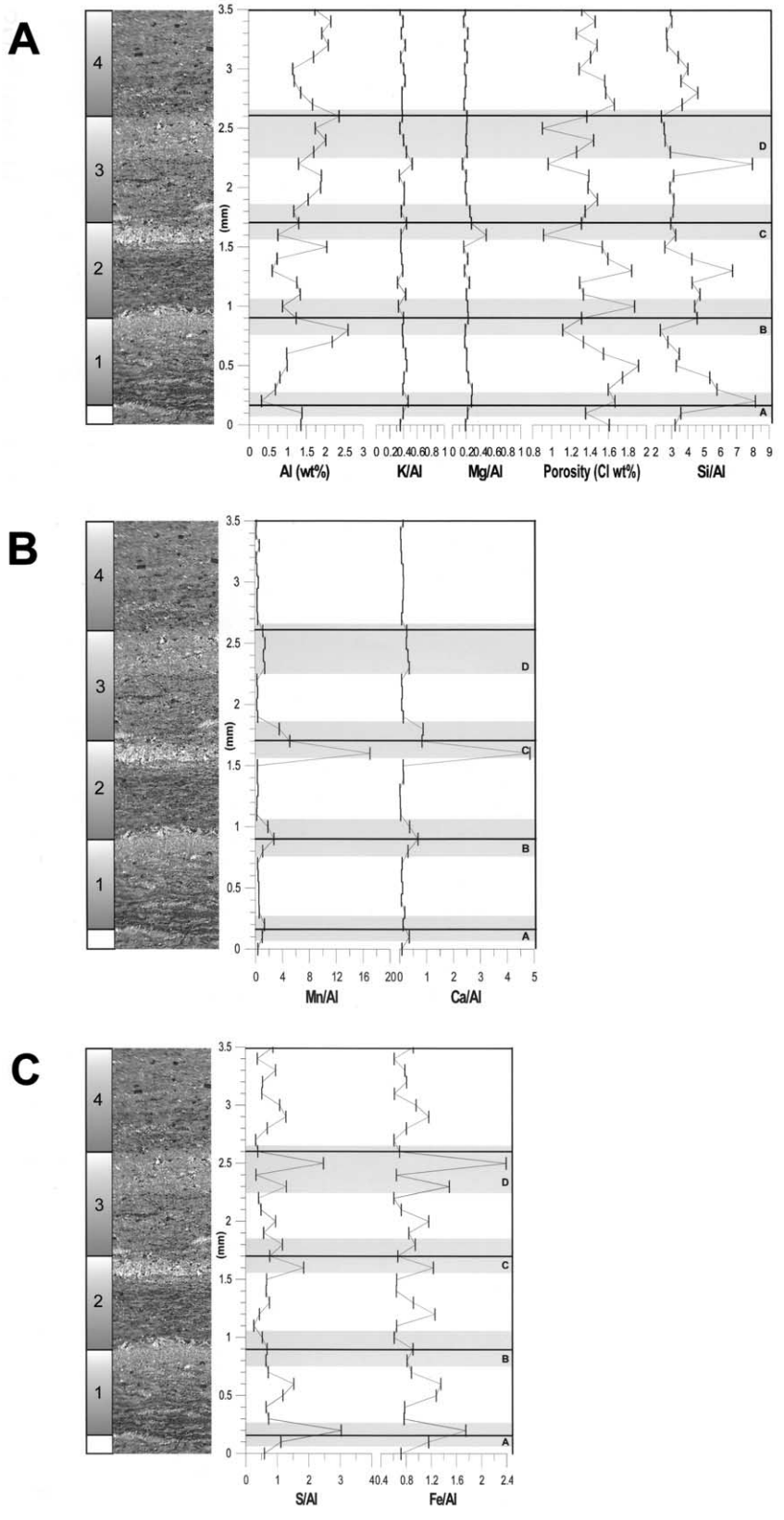

Fig. 3. High-magnification (20×) backscattered electron image showing four varves, numbered 1 to 4, containing kutnahorite laminae (core depth, 126 cm). Major element distributions shown from EDS line raster scan taken along extreme left-hand side of BSEI image. (A) Al (wt%), K/Al, Mg/Al, porosity (Cl wt%), Si/Al. (B) Mn/Al, Ca/Al. (C) S/Al, Fe/Al. Kutnahorite laminae are denoted by gray bands A to D.

Table 3. Composition of kutnahorite phase from EDS spot analysis (n = 79).

Variable	Mn	Ca	Mg	Fe	S	C	O	Cl	Total
Mean (wt%)	36.34	8.14	0.71	0.00	1.16	16.84	34.83	0.41	98.42
Minimum (wt%)	23.11	2.41	0.21	0.00	0.30	7.73	22.14	0.08	—
Maximum (wt%)	49.99	14.64	4.40	0.20	4.36	39.37	41.00	1.86	—
Standard deviation	4.91	2.35	0.61	0.02	0.60	6.63	3.12	0.27	—

by invoking a process where benthic tests are present during kutnahorite formation and planktonics tests are not. Benthic foraminifera can only live in oxygenated bottom waters. This implies a link between periodic oxic events, where benthic foraminifera recolonize the formerly anoxic deeps and the formation of kutnahorite laminae, an association previously observed by Sohlenius et al. (1996b) and Huckriede and Meischner (1996).

Because planktonic foraminifera tests are found free of kutnahorite, they are almost certainly not present (with the benthic tests) during the kutnahorite formation period; therefore, an erosional origin for planktonic tests seems unlikely. This suggests that during Littorina times, when surface-water conditions are reported to have been more saline than at present (Sohlenius et al., 1996a), planktonic foraminifera may have lived in the Baltic Sea. This observation also implies that the primary period of kutnahorite formation is relatively short; otherwise, planktonic foraminifera tests would be expected to become encrusted in kutnahorite as they where buried in the sediments.

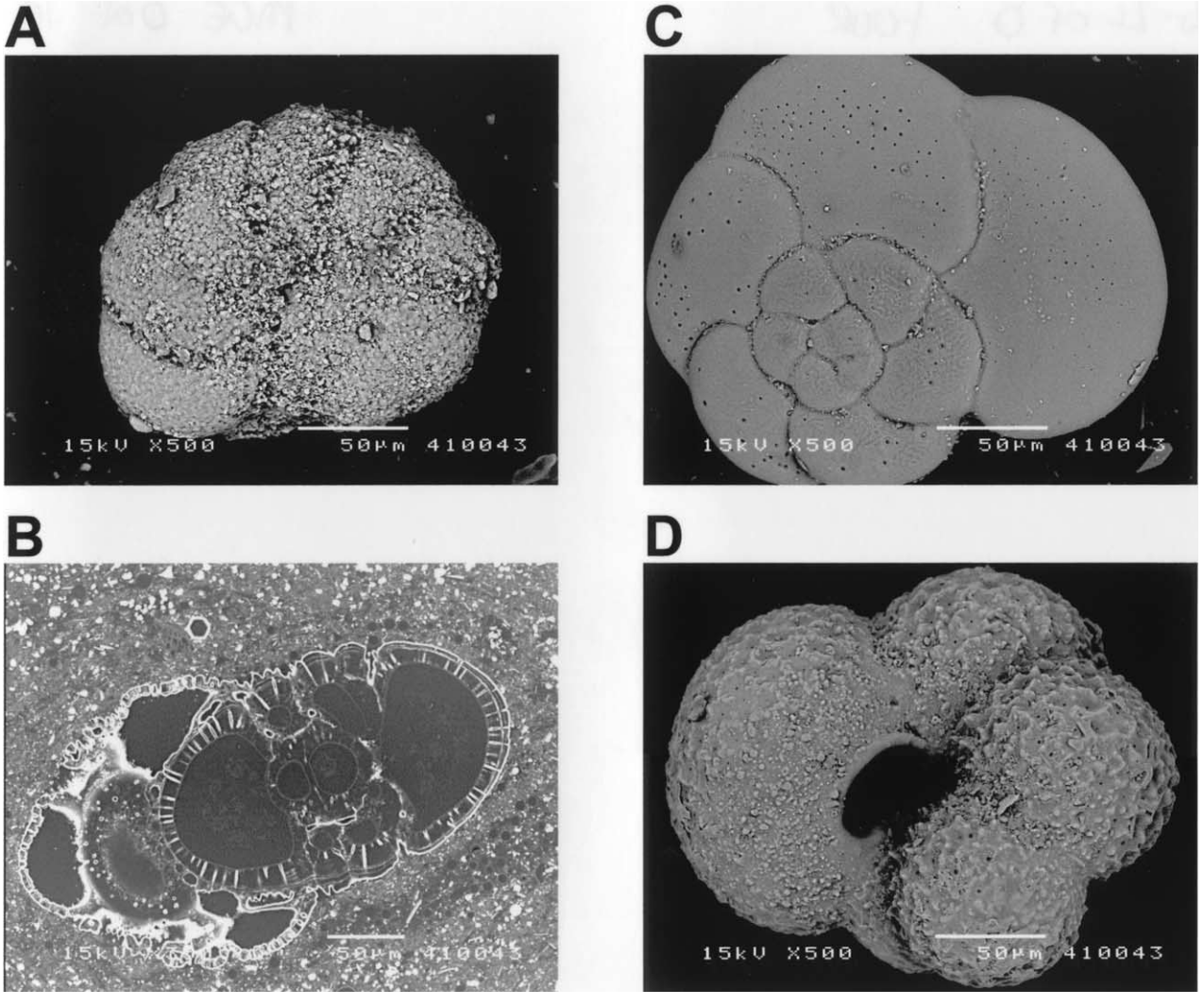

Fig. 4. (A) Benthic foraminifera *Elphidium excavatum* heavily encrusted in kutnahorite. (B) Backscattered electron image cross section of *E. excavatum*; bright outline is kutnahorite overgrowth. Overgrowth extends along pores in *E. excavatum* foraminiferal test. (C) Planktonic foraminifera *Globorotalia scitula*, with surface ornamentation similar to *E. excavatum* in life. (D) Right coiling planktonic foraminifera *Neogloboquadrina pachyderma.*

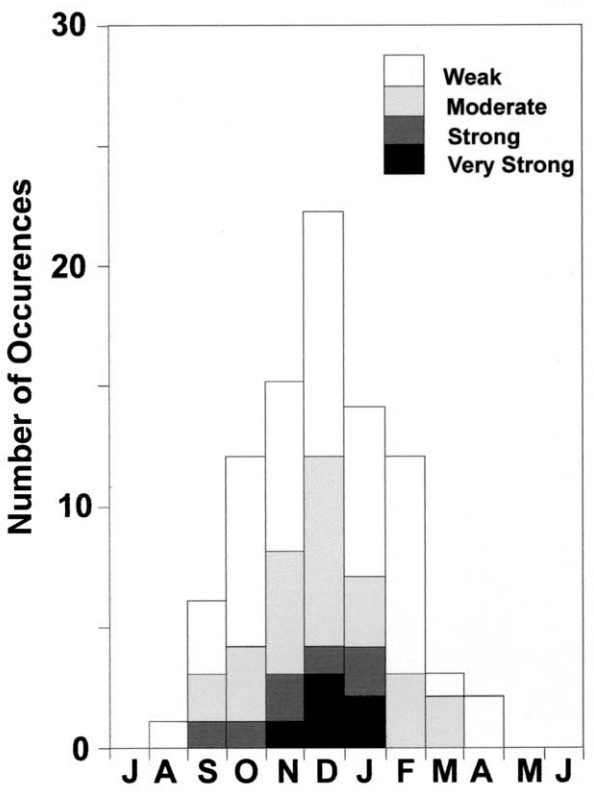

Fig. 5. Seasonal distribution and intensity of major Baltic inflows, predicted from historical records (after Matthäus and Schinke, 1994).

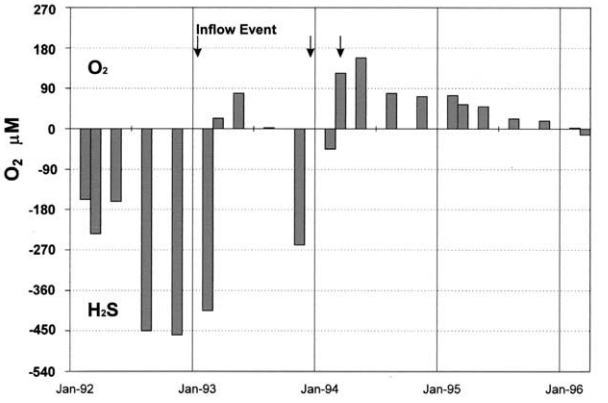

Fig. 6. Variations in bottom-water conditions (230 to 240 m) in the Gotland Deep from 1992 to 1996 (after Nehring et al., 1995b) and inflow events occurring at the Darss Sill. H_2S concentrations are plotted as negative O_2 concentrations.

4.4. Seasonality of Oxic Inflows

The only documented flushing of the Baltic deeps with oxygenated water occurs during episodic inflows of saline water, known as major Baltic inflows (Matthäus and Franck, 1992). A lightboat stationed in the Darss Strait has provided detailed data between 1880 and 1994 on the atmospheric and hydrologic conditions in the critical sill area (Matthäus, 1995). Matthäus and Franck (1992) used these data to estimate the timing of major inflows of saline water into the Baltic Sea during the 20th century. Figure 5 shows the extended winter season (August to April) when all major inflows occur. There is a normal distribution around a December maximum, but the strongest inflows only occur from November to January. However, because only the strongest inflows are likely to cause large changes in Gotland Deep conditions, the season where important inflows occur, in terms of Mn deposition, may be limited to the period November to January. In anoxic basins, Mn oxidation and deposition is believed to be rapid (2 to 3 d) after initial flushing with oxygenated water (Sternbeck and Sohlenius, 1997). It should therefore be the timing of first intrusion of saline water that controls Mn-oxide deposition.

Changes in Gotland Deep bottom-water conditions from 1992 to 1996 (Fig. 6) show the effects of oxic inflows occurring during that period. In January 1993, a major Baltic inflow occurred at the Darss Sill, but inflowing water was not observed in the Gotland Deep until March–April 1993 (Matthäus and Lass, 1995) because inflowing water must fill and overflow the smaller Arkona and Bornholm Basins (50 and 150 km from the Darss Sill area) before flowing over 400 km along the Stolpe Channel to the Gotland Deep. In 1994, however, because the Bornholm basin was already filled with dense saline water from the 1993 event, two small inflow events that occurred during December and March flowed rapidly (less than 1 month) to the Gotland Deep, causing bottom water with $[H_2S] > 180$ μM to be replaced rapidly with inflowing waters with $[O_2] > 130$ μM (Matthäus and Lass, 1995; Nehring et al., 1995a). Therefore, depending on variation in conditions in the approaches to the Gotland Deep, there is a variable delay of 1 to 4 months from the initial inflow at the Darrs Sill until a change in Gotland Deep water column conditions is measurable. Mn-oxide deposition is therefore likely to be seasonal, with deposition occurring between early February and late May, depending on the timing of the inflow event and the prevailing condition in the Baltic's deep basins.

A solid-phase Mn enrichment was observed in surface sediments sampled in 1994 equivalent to the amount of Mn^{2+} stored in anoxic bottom waters in 1992 before the 1993 inflow event (Brügmann et al., 1997; Heiser et al., 2001), showing that manganese deposition occurred as a result of these inflow events.

Burke et al. (2002) and section 4.2 of this study demonstrate that kutnahorite laminae occur as late winter–early spring deposits relative to varves. This timing information from varves is consistent with evidence of the timing of the first arrival of saline inflows in the Gotland Deep, which implies a direct causal link between the deposition of Mn-oxide laminae and major Baltic inflow occurrence.

4.5. Microfabric of Rhodochrosite Laminae

SEM allows the fine-scale structure of the kutnahorite laminae to be discerned (Figs. 7A–D). Kutnahorite laminae commonly consist of aggregates of 2- to 10-μm globular crystallites. Under BSEI, kutnahorite laminae appear as a bright bands of crystallites, always occurring as a parallel overprint to other clay-rich and diatomaceous laminae. In many cases, a diffuse region of 2- to 3-μm bright framboidal or cubic pyrite crystals

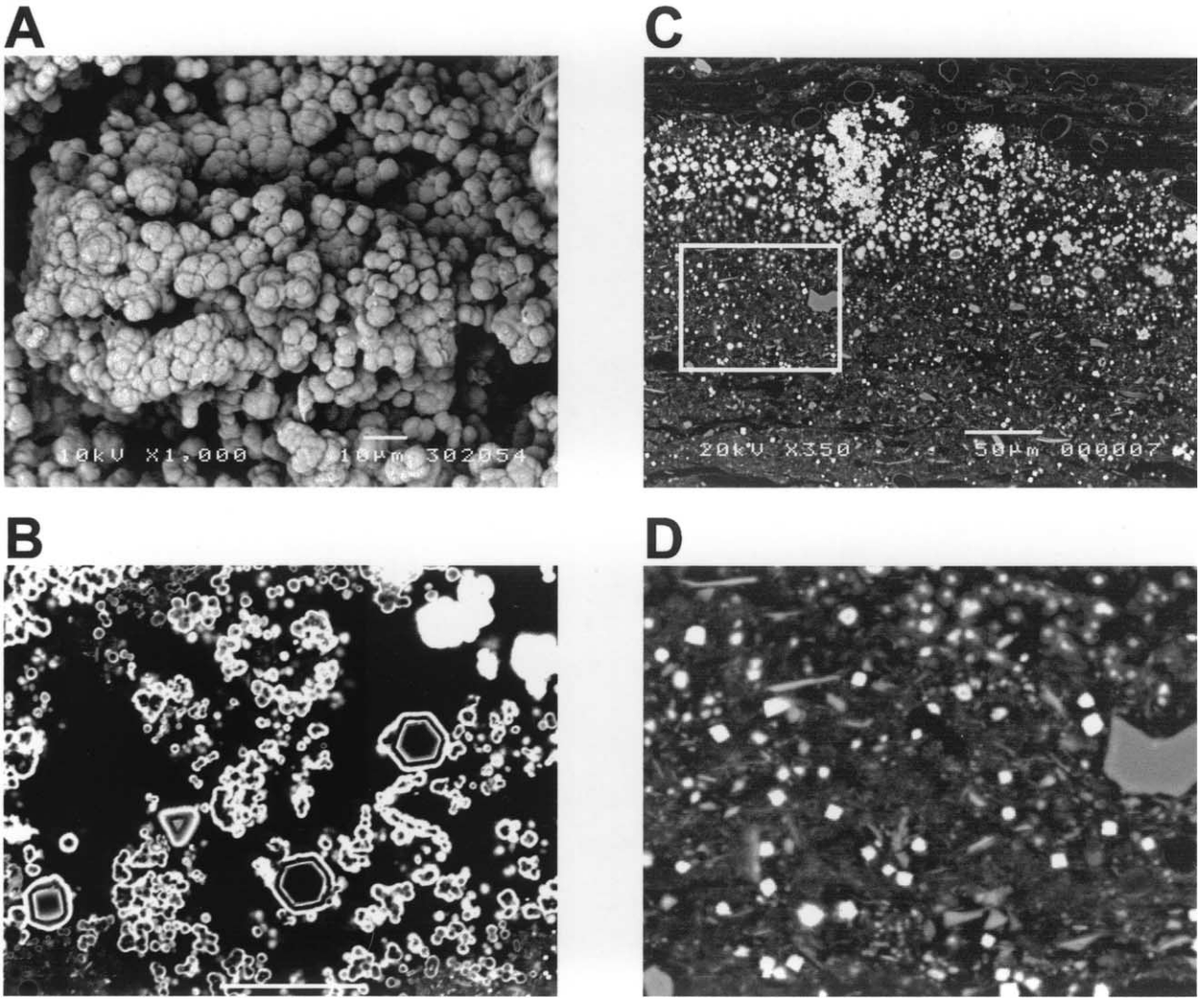

Fig. 7. (A) Topographical SEM image of aggregate of globular kutnahorite crystallites. (B) Backscattered electron image of hexagonal kutnahorite crystals (pseudomorphs of γ-Mn-sulfide) in ground mass of globular crystallites. (C) Backscattered electron image with kutnahorite laminae showing as a bright band of crystallites with a zone of diffuse small (>1 μm) cubic pyrite crystallites beneath; shown in detail in (D).

occurs below the kutnahorite laminae. The occurrence of cubic pyrite is limited only to areas associated with kutnahorite laminae, but framboidal pyrite is commonly found elsewhere in Littorina sediments. In Landsort Deep sediments, Böttcher and Lepland (2000) associated single pyrite framboids with Fe-sulfide formation within the water column, and clusters of framboidal pyrite, which include euhedral crystals, with Fe-sulfide formation within the sediments. In Jurassic mudstones, Taylor and Macquaker (2000) attributed framboidal pyrite to early formation under highly sulfidic conditions and euhedral pyrite to slower formation under less reducing conditions. These pyrite sublayers are therefore likely to have formed within the sediments, and the sublayers possibly reflect a redox-dependent distribution of Fe during kutnahorite formation.

Hexagonal kutnahorite crystals (20 to 30 μm) have been observed within or at the base of 12 (13%) of the 95 kutnahorite laminae observed from 118 to 143 cm. These crystals have a hollow core and are almost certainly pseudomorphs of hexagonal manganese sulfide because they are consistent with the γ-Mn-sulfide crystal morphologies reported previously in Baltic sediments, both in the Landsort Deep (Baron and Debyser, 1957; Debyser, 1961; Suess, 1979; Lepland and Stevens, 1998) and in the Gotland Deep (Böttcher and Huckriede, 1997). The occurrence of these pseudomorphs implies a complex sequence of environmental conditions (Fig. 8).

4.5.1. Formation of Mn-Sulfide

To form pseudomorphs as shown in Figure 7B, initially, Mn-sulfide crystals must have grown (Fig. 8A) after deposition of a Mn-oxide lamina. The precipitation of Mn-sulfide in preference to Mn-carbonate requires a high excess of free sulfide relative to alkalinity and an environment completely depleted in Fe, which would otherwise preferentially react with sulfide to form Fe-sulfides (Böttcher and Huckriede, 1997). The site of maximum bacterial sulfate reduction rates in Gotland Deep

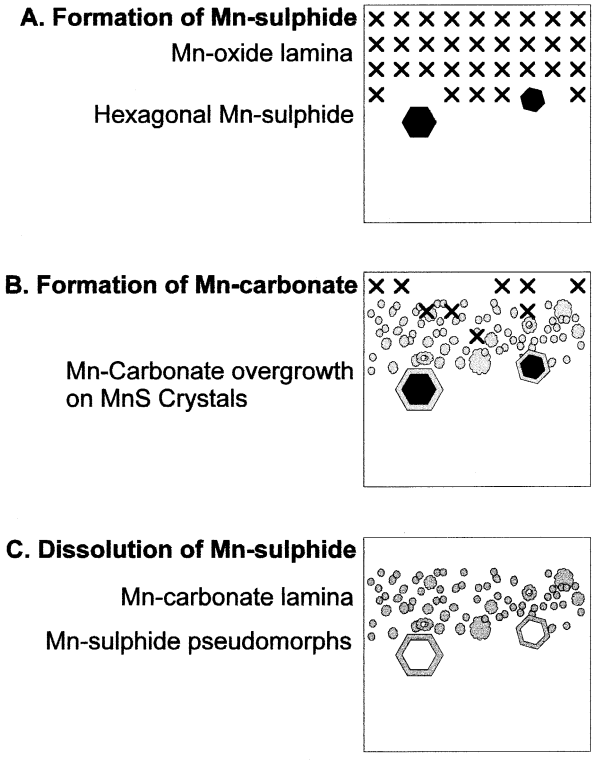

Fig. 8. Mn-sulfide pseudomorph formation sequence.

sediments has been observed by Piker et al. (1998) at between 10 to 20 cm below the sediment–water interface. High in situ H_2S and alkalinity concentrations should therefore be present below the Mn-oxide lamina. Large amounts of Mn^{2+} can be produced rapidly (Aller, 1980) by bacterial Mn reduction (and possibly by direct chemical reduction) of the Mn-oxide lamina; hence, large concentrations of free Mn^{2+} will be present at the sediment–water interface. The likely site of Mn-sulfide precipitation is therefore at the base of the Mn-oxide lamina, where high Mn^{2+} is met by high concentrations of H_2S diffusing upward from the site of maximum bacterial sulfate reduction.

4.5.2. Formation of Mn-Carbonate

After initial Mn-sulfide growth, conditions must have altered sufficiently so that kutnahorite overgrows on the Mn-sulfide crystals where produced (Fig. 8B). Alkalinity is produced as a result of bacterial reduction of the Mn-oxide laminae, and simultaneously, H_2S will be consumed by formation of Mn-sulfide. As a result, alkalinity can eventually become locally in excess relative to H_2S, and conditions may change to favor kutnahorite precipitation, both as an overgrowth on the hexagonal Mn-sulfide crystals and in separate kutnahorite crystallites.

The banding evident in the pseudomorphs (Fig. 7B), suggests that the precise precipitation microhabitat of the pseudomorphs may alternate between Mn-sulfide and kutnahorite formation, depending on subtle lamina-scale variations in both the production and diffusion of H_2S and alkalinity.

4.5.3. Dissolution of Mn-Sulfide

After all the Mn-oxide lamina has been consumed, the source of excess in situ Mn^{2+} will no longer be present, and no further kutnahorite or Mn-sulfide can be formed as a result of this mechanism. To leave hollow Mn-sulfide pseudomorphs (Fig. 8C), therefore, the early-formed Mn-sulfide almost certainly will have become unstable and dissociated. Because Mn-sulfide crystals have only been observed once previously in Gotland Deep sediments (Böttcher and Huckriede, 1997), it seems that Mn-sulfide preservation is not typical—indeed, the long-term sedimentary pore-water conditions in the Gotland Deep have been commonly reported to be oversaturated (or metastable) with respect kutnahorite, but undersaturated with respect to Mn-sulfide (Kulik et al., 2000; Heiser et al., 2001). Mn-sulfide will therefore normally tend to dissociate and diffuse away into anoxic pore waters. The resultant kutnahorite lamina containing Mn-sulfide pseudomorphs will then record both the deposition of an ephemeral Mn-oxide lamina and the sensitive changes in geochemical conditions during kutnahorite formation.

5. CONCLUSIONS

SEM images have revealed the occurrence of kutnahorite overgrowth solely on benthic and not on planktonic foraminifera tests. This strongly implies a link between oxic bottom-water conditions and kutnahorite formation.

EDS combined with backscatter electron imagery enables the placement of kutnahorite laminae within an annual cycle of deposition, showing that kutnahorite deposition is a rapid phenomenon occurring on seasonal timescales. The occurrence of kutnahorite only as a winter–early spring deposit is in close agreement with the seasonality of flushing of the Gotland Deep as recorded in historical records. This finding provides supporting evidence for the assumed direct causal link between saline inflow events and kutnahorite deposition and suggests that this has been a regular feature sedimentation throughout the Holocene sediments of the Gotland Deep.

The relatively common occurrence of hexagonal γ-Mn-sulfide pseudomorphs suggests that highly sulfidic conditions favoring the early formation of Mn-sulfide was reached much more commonly during kutnahorite formation in the Gotland deep than previously reported.

Acknowledgments—This research was funded by the award of NERC studentship GT4/98/ES/266 to I.T.B. We thank Kay Emeis of the Institute of Baltic Research, Warnemünde, Germany, who provided core material that made this study possible, and Ulrick Struck, also of the Institute of Baltic Research, for sharing radiocarbon data. We thank John Thomson and Richard Pearce for their advice. We also extend special thanks to Eelco Rohling and John Murray for their help in foraminiferal identification. An earlier draft of this manuscript was greatly improved by prereview comments from Chris German. We thank Steve Calvert, David Burdige, and an anonymous reviewer for their time and helpful comments.

Associate editor: D. J. Burdige

REFERENCES

Aller R. C. (1980) Diagenetic processes near the sediment–water interface of Long Island Sound II: Fe and Mn. *Adv. Geophys.* **22,** 351–415.

Baron G. and Debyser J. (1957) Sur la presence dans les vases or-

ganiques de la mer Baltique du sulfure manganeux b hexagonal. *C. R. Acad. Sci. Paris* **245,** 1148–1150.

Berner R. A. (1981) A new geochemical classification of sedimentary environments. *J. Sediment. Petrol.* **51,** 0359–0365.

Björck S. (1995) A review of the history of the Baltic Sea. *Quat. Int.* **27,** 19–40.

Björck S., Kromer B., Johnsen S., Bennike O., Hammarlund D., Lemdahl G., Possnert G., Rasmussen T. L., Wohlfarth B., Hammer C. U., and Spurk M. (1996) Atmospheric deglacial records around the North Atlantic. *Science* **274,** 1155–1160.

Boesen C. and Postma D. (1988) Pyrite formation in anoxic environments of the Baltic. *Am. J. Sci.* **288,** 575–603.

Böttcher M. E. (1998) Manganese(II) partitioning during experimental precipitation of rhodochrosite–calcite solid solutions from aqueous solutions. *Mar. Chem.* **62,** 287–297.

Böttcher M. E. and Huckriede H. (1997) First occurrence and stable isotope composition of authigenic g-MnS in the central Gotland Deep (Baltic Sea). *Mar. Geol.* **137,** 201–205.

Böttcher M. E. and Lepland A. (2000) Biogeochemistry of sulfur in a sediment core from the west-central Baltic Sea: Evidence from stable isotopes and pyrite textures. *J. Marine Syst.* **25,** 299–312.

Brodie I. and Kemp A. E. S. (1994) Variation in Biogenic and Detrital Fluxes and Formation of Laminae in Late Quaternary Sediments from the Peruvian Coastal Upwelling Zone. *Mar. Geol.* **116,** 385–398.

Brodniewicz I. (1965) Recent and some Holocene foraminifera of the Southern Baltic Sea. *Acta Palaeontol.*Pol. **10,** 131–233.

Brügmann L., Halberg R., Larsson C., and Löffler A. (1997) Changing redox conditions in the Baltic Sea deep basins: Impacts of concentration and speciation of trace metals. *Ambio* **26,** 107–112.

Burke I. T., Grigorov I., and Kemp A. E. S. (2002) Micro-fabric study of diatomaceous and lithogenic deposition in laminated sediments from the Gotland Deep, Baltic Sea. *Mar. Geol.* In press.

Calvert S. E. and Price N. B. (1970) Composition of manganese nodules and manganese carbonates from Loch Fyne, Scotland. *Contrib. Mineral. Petrol.* **29,** 215–233.

Calvert S. E. and Pedersen T. F. (1993) Geochemistry of recent oxic and anoxic marine sediments: Implications for the geological record. *Mar. Geol.* **113,** 67–88.

Calvert S. E. and Pedersen T. F. (1996) Sedimentary geochemistry of manganese: Implications for the environment of formation of manganiferous black shales. *Econ. Geol.* **91,** 36–47.

Calvert S. E., Pedersen T. F., and Karlin R. E. (2001) Geochemical and isotopic evidence for post-glacial palaeoceanographic changes in Saanich Inlet, British Columbia. *Mar. Geol.* **174,** 287–305.

Danyushevskaya A. I. (1992) Geochemistry of organic matter in bottom sediments of the Baltic Sea. *Oceanology* **32,** 469–475.

Debyser J. (1961) *Contribution à l'étude géochimique des vases marine.* PhD Thesis, Institute Francais Du Petrole, Paris. 249 p.

Dyrssen D. and Kremling K. (1990) Increasing hydrogen sulphide concentration and trace metal behaviour in the anoxic Baltic waters. *Mar. Chem.* **30,** 193–204.

Emeis K. C. and Struck U. (1998) Gotland Deep Experiment (GOBEX). Status report on investigations concerning benthic processes, sediment formation and accumulation. *Meereswissenschaftliche Berichte, Warnemünde* **34.**

Fan D., Lui T., and Ye J. (1992) The process of formation of manganese carbonate deposits hosted in black shale series. *Econ. Geol.* **87,** 65–67.

Froelich P. N., Klinkhammer G. P., Bender M. L., Luedtke N. A., Heath G. R., Cullen D., Dauphin P., Hammond D., Hartman B., and Maynard V. (1979) Early oxidation of organic matter in pelagic sediments of the eastern equatorial atlantic: Suboxic diagenesis. *Geochim. Cosmochim. Acta* **43,** 1075–1090.

Hein J. R. and Koski R. A. (1987) Bacterially mediated diagenetic origin for chert-hosted manganese deposits in the Franciscan Complex, California Coast Ranges. *Geology* **15,** 722–726.

Heiser U., Neumann T., Scholten J., and Stüben D. (2001) Recycling of manganese from anoxic sediments in stagnant deeps by seawater inflow: A study of surface sediments from the Gotland Basin, Baltic Sea. *Mar. Geol.* **177,** 151–166.

Huckriede H. and Meischner D. (1996) Origin and environment of manganese-rich sediments within black shale deeps. *Geochim. Cosmochim. Acta* **60,**1399–1413.

Ignatius H., Axberg S., Niemistö L., and Winterhalter B. (1981) Quaternary geology of the Baltic Sea. In *The Baltic Sea*(ed. A. Voipio), pp. 54–104. Elsevier.

Jakobsen R. and Postma D. (1989) Formation and solid solution behaviour of Ca-rhodochrosites in marine muds of the Baltic Deeps. *Geochim. Cosmochim. Acta* **53,** 2639–2648.

Jenkyns H. C., Géczy B., and Marshall J. D. (1991) Jurassic manganese carbonates of central Europe and the early Toarcian anoxic event. *J. Geol.* **99,** 137–149.

Kabailiené M. (1995) The Baltic Ice Lake and Yoldia Sea stages, based on data from diatom analysis in the central, south-eastern and eastern Baltic. *Quat. Int.* **27,** 69–72.

Kemp A. E. S., Pearce R. B., Pike J., and Marshall J. E. A. (1998) Microfabric and microcompositional studies of Pliocene and Quaternary sapropels from the eastern Mediterranean. *Proc. ODP Sci. Res.* **160,** 349–364.

Kemp A. E. S., Pearce R. B., Koizumi I., Pike J., and Rance S. J. (1999) The role of mat-forming diatoms in the formation of Mediterranean sapropels. *Nature* **398,** 57–61.

Kremling K. (1983) The behaviour of Zn, Cd, Cu, Ni, Co, Fe, and Mn in anoxic Baltic waters. *Mar. Chem.* **13,** 87–108.

Kulik D. A., Kersten M., Heiser U., and Neumann T. (2000) Application of. Gibbs energy minimization to model early-diagenetic solid-solution aqueous-solution equilibria involving authigenic rhodochrosites in anoxic Baltic Sea sediments. *Aquat. Geochem.* **6,** 147–199.

Lepland A. and Stevens R. L. (1998) Manganese authigenesis in the Landsort Deep, Baltic Sea. *Mar. Geol.* **151,** 1–25.

Matthäus W. (1990) Mixing across the primary Baltic halocline. *Beitr. Meereskd.* **61,** 21–31.

Matthäus W. (1995) Natural variability and human impacts reflected in long-term changes in the Baltic deep water conditions—A brief review. *Dtsch. Hydrogr. Z.* **47,** 47–65.

Matthäus W. and Franck H. (1992) Characteristics of major Baltic inflows—A statistical analysis. *Cont. Shelf Res.* **12,** 1375–1400.

Matthäus W. and Schinke H. (1994) Mean atmospheric circulation patterns associated with major Baltic inflows. *Dtsch. Hydrogr. Z.* **46,** 321–399.

Matthäus W. and Lass H. U. (1995) The Recent Salt Inflow into the Baltic Sea. *J. Phys. Oceanogr.* **25,** 280–286.

Mörner N. A. (1995) The Baltic Ice Lake–Yoldia Sea transition. *Quat. Int.* **27,** 95–98.

Nehring D., Matthaus W., Lass H. U., Nausch G., and Nagel K. (1995a) The Baltic Sea 1994—Consequences of the hot summer and inflow events. *Dtsch. Hydrogr. Z.* **47,** 131–144.

Nehring D., Matthaus W., Lass H. U., Nausch G., and Nagel K. (1995b) The Baltic Sea in 1995—Beginning of a new stagnation period in its central deep waters and decreasing nutrient load in its surface layer. *Dtsch. Hydrogr. Z.* **47,** 319–327.

Neumann T., Christiansen C., Clasen S., Emeis K. C., and Kunzendorf H. (1997) Geochemical records of salt-water inflows into the deeps of the Baltic Sea. *Cont. Shelf Res.* **17,** 95–115.

Okita P. M., Maynard J. B., Spiker E. C., and Force E. R. (1988) Isotopic evidence for organic matter oxidation by manganese reduction in the formation of stratiform manganese carbonate ore. *Geochim. Cosmochim. Acta* **52,** 2679–2685.

Pedersen T. F. and Price N. B. (1982) The Geochemistry of manganese carbonate in Panama basin sediments. *Geochim. Cosmochim. Acta* **46,** 59–68.

Pike J. and Kemp A. E. S. (1996) Preparation and analysis techniques for studies of laminated sediments. *Palaeoclimatology and Palaeoceanography from Laminated Sediments* (ed. A. E. S. Kemp), pp. 37–48.Special Publication 116. Geological Society of London.

Pike J. and Kemp A. E. S. (1999) Diatom mats in Gulf of California sediments: Implications for the paleoenvironmental interpretation of laminated sediments and silica burial. *Geology* **27,** 311–314.

Piker L., Schmaljohann R., and Imhoff F. (1998) Dissimilatory sulfate reduction and methane production in Gotland Deep sediments (Baltic Sea) during a transition from oxic to anoxic bottom water (1993–1996). *Aquat. Microb. Ecol.* **14,** 183–193.

Raukas A. (1995) Evolution of the Yoldia Sea in the eastern Baltic. *Quat. Int.* **27,** 99–102.

Schinke H. and Matthäus W. (1998) On the causes of major Baltic inflows—An analysis of a long time series. *Cont. Shelf Res.* **18,** 67–97.

Sohlenius G., Sternbeck J., Anden E., and Westman P. (1996a) Holocene history of the Baltic Sea as recorded in a sediment core from the Gotland Deep. *Mar. Geol.* **134,** 183–201.

Sohlenius G., Wastegård S., and Sternbeck J. (1996b) Evidence of benthic colonisation during formation of laminated sediments in the Gotland Deep, Baltic Sea. *Quaternaria* **A,** paper IV.

Sternbeck J. (1997) Kinetics of rhodochrosite crystal growth at 25°C: The role of surface speciation. *Geochim. Cosmochim. Acta* **61,** 785–793.

Sternbeck J. and Sohlenius G. (1997) Authigenic sulphide deposits and carbonate mineral formation in Holocene sediments of the Baltic Sea. *Chem. Geol.* **135,** 55–73.

Suess E. (1979) Mineral phases formed in anoxic sediments by microbial decomposition of organic matter. *Geochim. Cosmochim. Acta* **43,** 337–352.

Taylor K. G. and Macquaker J. H. S. (2000) Early diagenetic pyrite morphology in a mudstone-dominated succession: The Lower Jurassic Cleveland Ironstone Formation, Eastern England. *Sediment. Geol.* **131,** 77–86.

Thomson J., Higgs N. C., Jarvis I., Hydes S., Colley S., and Wilson T. R. S. (1986) The behaviour of manganese in Atlantic carbonate sediments. *Geochim. Cosmochim. Acta* **50,** 1807–1818.

Wastegård S., Andrén T., Sohlenius G., and Sandgren P. (1995) Different phases of the Yoldia Sea in the north-western Baltic Proper. *Quat. Int.* **27,** 121–129.

Xu X., Huang H., and Liu B. (1990) Manganese deposits of the Proterozoic Datangpo Formation, South China: Genesis and paleogeography. *Int. Assoc. Sedimentol. Spec. Publ.* **11,** 39–50.

Zenkevitch L. (1963) *Biology of the Seas of the USSR*. Allen and Unwin.